7072 *Inorg. Chem.* **2010**, *49*, 7072–7079
DOI: 10.1021/ic100862y

Inorganic Chemistry
Article

New Ru(II) Complexes with Anionic and Neutral N-Donor Ligands as Epoxidation Catalysts: An Evaluation of Geometrical and Electronic Effects

Mohamed Dakkach,[†,∥] M. Isabel López,[†] Isabel Romero,*[,†] Montserrat Rodríguez,*[,†] Ahmed Atlamsani,[∥] Teodor Parella,[§] Xavier Fontrodona,[†] and Antoni Llobet[‡,§]

[†]*Departament de Química i Serveis Tècnics de Recerca, Universitat de Girona, Campus de Montilivi, E-17071 Girona, Spain,* [‡]*Institute of Chemical Research of Catalonia (ICIQ), Av. Països Catalans 16, E-43007 Tarragona, Spain,* [§]*Departament de Química i Servei de RMN Universitat Autònoma de Barcelona, Cerdanyola del Vallès, E-08193 Barcelona, Spain, and* [∥]*Laboratoire de Physico-Chimie des Interfaces et Environnement, Département de Chimie, Faculté des Sciences, Université Abdelmalek Essaadi, B.P.: 2121 93000 Tétouan, Morocco*

Received May 2, 2010

The synthesis of a family of new Ru complexes containing the meridional trpy ligand with general formula $[Ru^{II}(T)(D)(X)]^{n+}$ (T = 2,2′:6′,2″-terpyridine (trpy); D = 3,5-dimethyl-2-(2-pyridyl)pyrrolate (pyrpy), and 2-(1-Methyl-3-pyrazolyl)pyridine (pypz-Me); X = Cl, H_2O) have been described. All complexes have been spectroscopically characterized in solution through ^1H NMR and UV−vis techniques, and the chloro complexes have also been characterized in the solid state through monocrystal X-ray diffraction analysis. The pyrpy ligand undergoes an oxidation at the 3-position of the pyrrolate ring during the formation of the corresponding aqua complex thus generating the analogous compound containing the oxidized ligand pyrpy-O. The redox properties of all complexes have also been studied by means of CV and DPV techniques, where both geometrical (*trans* vs *cis*) and electronic (neutral vs anionic) effects can be unveiled and rationalized. Finally, the reactivity of the whole set of Ru-OH_2 complexes has been tested with regard to the epoxidation of different alkenes with $PhI(OAc)_2$. In all cases good selectivities and conversions were obtained. Furthermore, total retention of the initial *cis* configuration was achieved when using these catalysts to epoxidize *cis*-β-methylstyrene.

Introduction

Ruthenium polypyridyl complexes have been extensively studied over the years because they enjoy a combination of unique chemical, electrochemical, and photochemical properties[1,2] that has allowed the exploration of a wide variety of fields including bioinorganic chemistry[3] and catalysis.[4]

In the particular field of redox catalysis, the relationship between performance and structure of a catalyst is further complicated by the presence of multiple redox state species involved in the catalytic cycle. Therefore, the thermodynamic and kinetic characterization of the reactions that undergo the different oxidation state species of a particular catalyst is of paramount importance to understand and optimize catalyst performance.

A particularly interesting family of redox catalysts is the so-called Ru-OH_2 type of complexes. These Ru-aquo complexes can easily lose protons and electrons and reach higher oxidation states as exemplified below, where L5 represent polypyridylic type of ligands,

$$L_5Ru^{II}\text{-}OH_2 \underset{+H^+ + e^-}{\overset{-H^+ - e^-}{\rightleftharpoons}} L_5Ru^{III}\text{-}OH \underset{+H^+ + e^-}{\overset{-H^+ - e^-}{\rightleftharpoons}} L_5Ru^{IV}{=}O \quad (1)$$

The sequential loss of protons and electrons allows to easily reach reactive Ru^{IV}=O species, and as a consequence they have been widely used as redox catalysts for the oxidation of both organic and inorganic substrates. A large amount of literature has emerged during the past two decades

*To whom correspondence should be addressed. E-mail: marisa.romero@udg.edu (I.R.); montse.rodriguez@udg.edu (M.R.).

(1) (a) Lappin, A. G.; Marusak, R. A. *Coord. Chem. Rev.* **1991**, *109*, 125–180. (b) Griffith., W. P. *Chem. Soc. Rev.* **1992**, *21*, 179–185. (c) Wing-Sze Hui, J.; Wong, W.-T. *Coord. Chem. Rev.* **1998**, *172*, 389–436. (d) Clarke, M. J. *Coord. Chem. Rev.* **2002**, *232*, 69–93. (e) Meyer, T. J.; Huynh, M. H. V. *Inorg. Chem.* **2003**, *42*, 8140–8169.

(2) (a) Balzani, V.; Juris, A. *Coord. Chem. Rev.* **2001**, *211*, 97–115. (b) Sauvage, J.-P.; Collins, J.-P.; Chambron, J.-C.; Guillerez, S.; (c) Coudret, C.; Balzani, V.; Barigelletti, F.; De Cola, L.; Fannigni, L. *Chem. Rev.* **1994**, *94*, 993–1019. (d) Meyer, T. J. *Acc. Chem. Res.* **1989**, *22*, 163.

(3) (a) Kelly, S. O.; Barton, J. K. *Science* **1999**, *238*, 375. (b) Hall, D. B.; Holmlin, R. E.; Barton, J. K. *Nature* **1996**, *384*, 731. (c) Burrows, C. J.; Muller, J. G. *Chem. Rev.* **1998**, *98*, 1109. (d) Weatherly, S. C.; Yang, I. V.; Thorp, H. H. *J. Am. Chem. Soc.* **2001**, *123*, 1236.

(4) (a) Murahashi, S. I.; Takaya, H.; Naota, T. *Pure Appl. Chem.* **2002**, *74*, 19–24. (b) Naota, T.; Takaya, H.; Murahashi, S.-I. *Chem. Rev.* **1998**, *98*, 2599–2660. (c) Rodríguez, M.; Romero, I.; Llobet, A.; Deronzier, A.; Biner, M.; Parella, T.; Stoeckli-Evans, H. *Inorg. Chem.* **2001**, *40*, 4150–4156. (d) Jauregui-Haza, U. J.; Dessoudeix, M.; Kalck, Ph.; Wilhelm, A. M.; Delmas, H. *Catal. Today* **2001**, *66*, 297–302.

Published on Web 07/02/2010

related to this system, mainly because of the rich oxidative properties of the Ru^{IV}=O species. In addition, the reaction mechanisms for the oxidation of several substrates by Ru^{IV}=O have been thoroughly described together with the establishment and optimization of catalytic processes.[5]

The redox potentials, and therefore the performance, of a Ru-OH_2 catalyst can be tuned through the ligands with the addition of electron donating or withdrawing groups. This is expected to respectively decrease and increase the Ru(IV)/Ru(III) and Ru(III)/Ru(II) redox potentials, and thus allows to generate a family of catalysts with a fine-tuned reactivity.[6] In addition to the electronic effects, examples also exist where sterically hindered ligands strongly influence the reactivity of a Ru=O system with regard to substrate oxidation.[7]

While a wide variety of Ru-OH_2 complexes containing neutral polypyridylic ligands has been described, the number of such complexes containing anionic ligands is much smaller.[8] Furthermore the number of Ru-OH_2 complexes with N-based anionic ligands is even more limited.[9]

In the present work we present the preparation, characterization, and catalytic performance of a new family of Ru-Cl and Ru-OH_2 complexes containing the meridional 2,2′:6′:2″-terpyridine (trpy) ligand and completing the octahedral coordination with non symmetric didentate ligands. The didentate ligands used are pyridylpyrrole (Hpyrpy) and pyrazolylpyridine (pypz-Me) that are depicted in Scheme 1. Upon deprotonation the Hpyrpy ligand is expected to coordinate in a chelating manner and exert a strong donation effect over the Ru center because of its anionic character.[10] On the other hand the non symmetric neutral pypz-Me ligand is expected to allow evaluation of steric effects depending on its mode of coordination toward the Ru center.[11,12] The catalytic performance of this new family of complexes has been tested with regard to the epoxidation of alkenes and is reported herein.

Results and Discussion

Synthesis and Crystal Structures. The synthetic strategy followed for the preparation of the complexes described in the present paper is outlined in Scheme 2. The nomenclature *trans* or *cis* for complexes refers to the relative

Scheme 1. Ligands Used in This Work

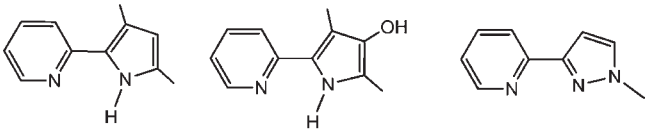

Hpyrpy Hpyrpy-O pypz-Me

position of the monodentate ligand (Cl or H_2O) with regard to the pyrrolate or pyrazole ring of the ligands pyrpy and pypz-Me, respectively.

The trichloro Ru complex [$Ru^{III}Cl_3$(trpy)], **1**, is used as starting material, followed by reduction with NEt_3. The didentate ligand, either pyrpy (previously deprotonated with NEt_3) or pypz-Me, is added to form the corresponding monochloro Ru(II) complexes, **2**, for the pyrpy case and a mixture of *trans* and *cis* isomers (*trans*-**4** and *cis*-**4**) for the pypz-Me case. The two isomers of complex **4** are easily separated through column chromatography. The exclusive formation of the *trans* isomer in **2** is not simple to explain though it must be due to electronic factors arising from the negative charge of the pyrrolate ring, since structural parameters are almost identical in the two families of complexes. No evidence for the existence of the other possible geometrical isomer has been obtained either in the solid state or in solution.

The Ru-OH_2 complexes *trans*-**3**, *trans*-**5**, and *cis*-**5** are easily obtained from the corresponding Ru-Cl complexes in the presence of Ag^+. However, for the case of complex **3** containing the pyrrolate ligand, the isolated Ru-aqua complex has experienced the oxidation of the carbon atom C23. This carbon is situated in between of the two methyl substituents of the pyrpy ligand, leading to the new anionic ligand pyrpy-O (scheme 1), as confirmed by NMR spectroscopy (see below).

It is worth mentioning here that whereas the two isomers of chloro complex **4** are stable to light irradiation in solution, their corresponding aqua complexes *trans*-**5** and *cis*-**5** are not. They undergo mutual isomerization under a constant intensity of white light irradiation, leading always to a *trans*/*cis* mixture of approximately 1.25:1. The ^{1}H NMR spectrum of the resulting mixture (obtained from *cis*-**5** irradiation) is shown in the Supporting Information.

The crystal structures of chloro complexes *trans*-**2**, *trans*-**4**, and *cis*-**4** have been solved by X-ray diffraction analysis. Figure 1 displays the molecular structures of the complexes whereas their main crystallographic data are reported in Table 1 and Supporting Information, Table S1. Selected bond distances and angles can be found in the Supporting Information, Tables S2 and S3.

In all cases, the Ru metal centers adopt an octahedrally distorted type of coordination where the trpy ligand is bonded in a meridional manner and the pyrpy and pypz-Me ligands act in a didentate fashion. The sixth coordination site is occupied by the chloro ligand. All bond distances and angles are within the expected values for this type of complexes.[13]

The comparison of *cis* versus *trans* geometries reveals significant differences in some structural parameters. For

(5) (a) Bryant, J. R.; Matsuo, T.; Mayer, J. M. *Inorg. Chem.* **2004**, *43*, 1587. (b) Sala, X.; Poater, A.; Romero, I.; Rodríguez, M.; Llobet, A.; Solans, X.; Parella, T.; Santos, T. M. *Eur. J. Inorg. Chem.* **2004**, 612. (c) Yip, W.-P.; Yu, W.-Y.; Zhu, N.; Che, C.-M. *J. Am. Chem. Soc.* **2005**, *127*, 14239. (d) Zong, R.; Thummel, R. P. *J. Am. Chem. Soc.* **2005**, *127*, 12802.

(6) (a) Llobet, A. *Inorg. Chim. Acta* **1994**, *221*, 125. (b) Szczepura, L. F.; Maricich, S. M.; See, R. F.; Churchill, M. R.; Takeuchi, K. J. *Inorg. Chem.* **1995**, *34*, 4198.

(7) Huynh, M. H. V.; Witham, L. M.; Lasker; Wetzler, M.; Mort, B.; Jameson, D. L.; White, P. S.; Takeuchi, K. J. *J. Am. Chem. Soc.* **2003**, *125*, 308.

(8) Dovletoglou, A.; Adeyemi, S. A.; Meyer, T. J. *Inorg. Chem.* **1996**, *35*, 4120.

(9) Fackler, N. L. P.; Zhang, S.; O'Halloran, T. V. *J. Am. Chem. Soc.* **1996**, *118*, 481–482.

(10) (a) Klappa, J. J.; Geers, S. A.; Schmidtke, S. J.; MacManus-Spencer, L. A.; McNeill, K. *Dalton Trans.* **2004**, 883–891. (b) Emmert; Brandl, F. *Ber. Chem.* **1927**, *60*, 2211. (c) Chiswell *Inorg. Chim. Acta* **1937**, *9*, 2024. (d) Pucci, D.; Aiello, I.; Aorea, A.; Bellusci, A.; Crispini, A.; Ghedini, M. *Chem. Commun.* **2009**, 1550–1552.

(11) Fusco, R. Pyrazoles, Pyrazolines, Pyrazolidines, Imidazoles and Condensed Rings. In *The Chemistry of Heterocyclic Compounds*; Wiley, R. H., Ed.; Interscience Publishers: New York, 1967; Vol. *22*, pp 1−174, .

(12) Thiel W. R.; Eppinger J. *Chem.—Eur. J.* **1997**, *3*. No. 5, 696.

(13) Sens, C.; Rodríguez, M.; Romero, I.; Parella, T.; Benet-Buchholz, J.; Llobet, A. *Inorg. Chem.* **2003**, *42*, 8385–8394.

Scheme 2. Synthetic Strategy

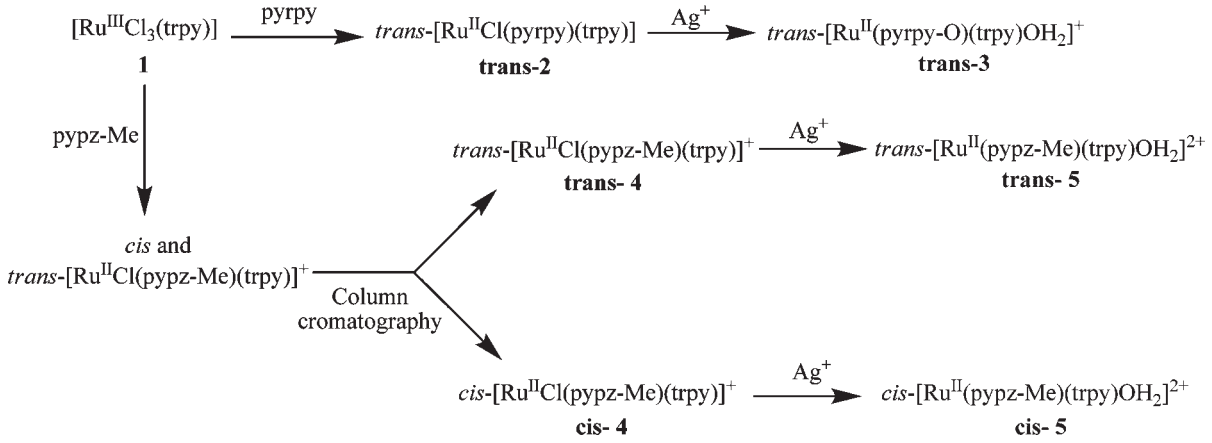

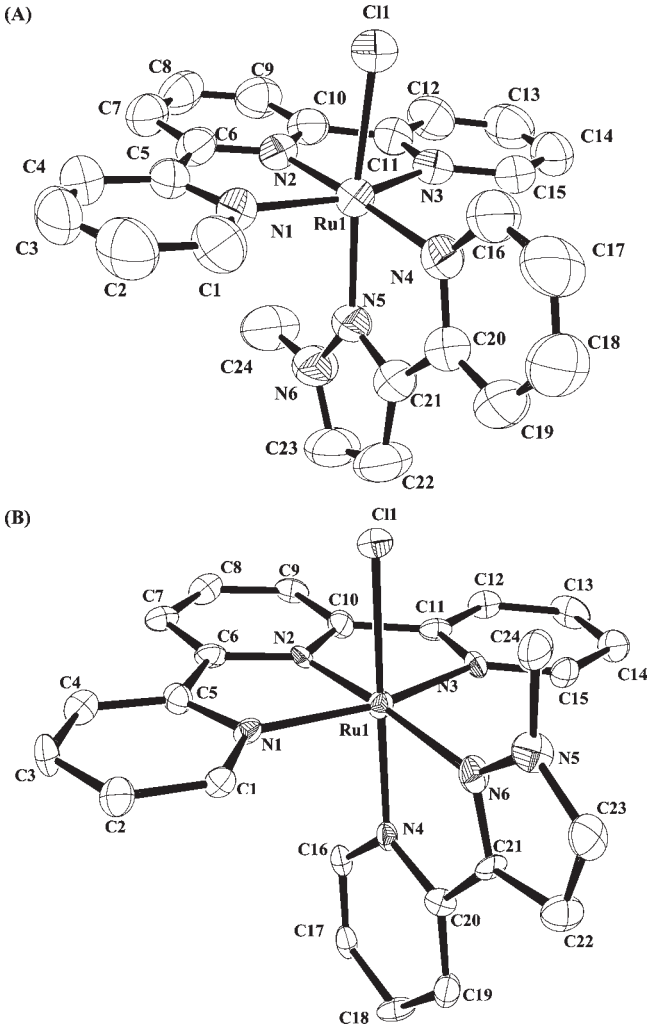

Figure 1. Ortep plot and labeling schemes for compounds (A) *trans*-**4** and (B) *cis*-**4**.

instance, it is interesting to note that the Ru−Cl bond length in *cis*-**4** complex, where the Cl atom is placed *trans* to the pyridyl N_{py} atom of pypz-Me, is larger (2.407 Å) than the analogous distance found in the *trans*-**4** complex (2.340 Å). In the latter case the Cl atom is *trans* to the pyrazole N_{pz} atom of the ligand, thus denoting the stronger *trans* influence of the pyridine ring with respect to the pyrazole. This effect is even larger in the case of the anionic pyrrolate ring in the *trans* complex **2**, with a Ru−Cl bond distance of 2.432 Å.

Table 1. Crystal Data for Compounds *trans*-**4** and *cis*-**4**[a]

	trans-**4**	*cis*-**4**
empirical formula	$C_{24}H_{20}ClF_6N_6PRu$	$C_{51}H_{46}Cl_8F_{12}N_{12}P_2Ru_2$
formula weight	673.95	1602.68
crystal system	triclinic	orthorhombic
space group	$P\bar{1}$	$Pca2(1)$
a [Å]	10.419(16)	15.863(5)
b [Å]	12.120(19)	13.625(4)
c [Å]	13.14(2)	28.230(8)
α [deg]	73.52(2)	90
β [deg]	67.41(2)	90
γ [deg]	83.96(3)	90
V [Å^3]	1469(4)	6102(3)
formula units/cell	2	4
temp, K	300(2)	100(2)
ρ_{calc}, [Mg/m^{-3}]	1.524	1.745
μ [mm^{-1}]	0.749	0.983
final R indices, [$I > 2\sigma(I)$]	$R_1 = 0.0559$ $wR^2 = 0.1370$	$R_1 = 0.0578$ $wR^2 = 0.1107$
R indices [all data]	$R_1 = 0.0949$ $wR^2 = 0.1544$	$R_1 = 0.1262$ $wR^2 = 0.1301$

[a] $R_1 = \sum||F_o| - |F_c||/\sum|F_o|$; $wR_2 = [\sum w(F_o^2 - F_c^2)^2/\sum w(F_o^2)^2]^{1/2}$, where $w = 1/[\sigma^2(F_o^2) + (0.0042P)^2]$ and $P = (F_o^2+2F_c^2)$.

The Cl−Ru−N *trans* angle in the complexes is also slightly dependent on the type of isomer. In complexes **2** and *trans*-**4**, the *trans* geometry allows the establishment of an intramolecular H-bond between the Cl ligand and the H(16) atom of the pyridyl ring of the didentate ligand (either pyrpy or pypz-Me; for *trans*-**4** the H(16)−Cl distance is 2.652 Å, the C(16)−Cl is 3.256 Å, and the angle Cl−H(16)−C(16) is 13.8°; see Figure 1), whereas this interaction is not present in the isomer *cis*-**4**. As a consequence, the *trans* bonding angle Cl(1)−Ru(1)−N(5) in complexes **2** and **4** is significantly smaller than 180° (172.3° and 170.4° for **2** and *trans*-**4**, respectively). Complex *cis*-**4** can only form such H-bonds through intermolecular interactions and this is manifested in the *zigzag* arrangement of the molecules in the crystal structure (see the Supporting Information, Figure S2).

Spectroscopic Properties. The one-dimensional (1D) and two-dimensional (2D) NMR spectra of all complexes were registered in d_6-acetone or D_2O and are presented in

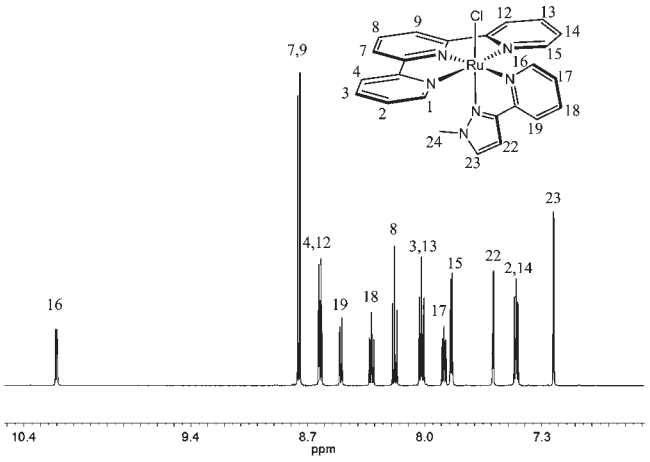

Figure 2. ^{1}H NMR spectrum of complex *trans*-**4**.

Figure 2 and in the Supporting Information. The absence of a resonance for H(23), expected to appear around 5−5.5 ppm in the ^{1}H NMR spectrum of complex *trans*-**3** (see the Supporting Information, Figure S5) confirms the oxidation of the pyrpy ligand during the synthesis, as described previously. The resonances found for all complexes are consistent with the structures obtained in the solid state.

The UV−vis spectra for both *trans*- and *cis*- isomers of complexes **4** and **5** are displayed in Figure 3, and those for **2** and **3** are gathered in the Supporting Information, Figure S10 together with a tentative assignment of the absorptions observed (Supporting Information, Table S4). The complexes exhibit ligand based $\pi-\pi^*$ bands below 350 nm and relatively intense bands above 350 nm mainly due to $d\pi-\pi^*$ MLCT transitions and also d-d transitions at lower energy.[14] For the Ru-Cl complexes the MLCT bands are shifted to the red with regard to the corresponding Ru-OH_2 species because of the relative destabilization of the $d\pi$(Ru) levels provoked by the anionic chloro ligand (compare for instance *trans*-**4** and *trans*-**5** spectra in Figure 3). A similar effect is also observed when comparing complexes containing the neutral pypz-Me or the anionic pyrpy ligand (complexes *trans*-**4** and **2** respectively, see Supporting Information).

Spectrophotometric acid−base titrations of the Ru-aquo complexes *trans*-**3**, *trans*-**5**, and *cis*-**5** were carried out to calculate their pK_a (eq 2, L = pypz-Me or pyrpy-O) which led to values of 9.75, 10.1, and 10.75, respectively. Isosbestic points confirming net conversion were found in all cases (for complex **3** at 340, 419, and 527 nm; for complex *trans*-**5** at 290, 320, 331, 425, and 486 nm; for complex *cis*-**5** at 317, 331, 341, 427, and 486 nm; see Supporting Information, Figure S11 for a detailed procedure description and spectra registered).

$$[Ru^{II}(L)(trpy)(H_2O)]^{n+} \xrightarrow[pK_{al}(Ru^{II})]{} [Ru^{II}(L)(trpy)(OH)]^{(n-1)+} + H^+ \quad (2)$$

The pK_a values for the Ru(III) oxidation states in all Ru-aquo complexes, which are discussed in the following section, were extracted from their Pourbaix diagrams (vide infra) and are displayed in Table 2 together with electrochemical information.

(14) Balzani, V.; Juris, A.; Veturi, M. *Chem. Rev.* **1996**, *96*, 759.

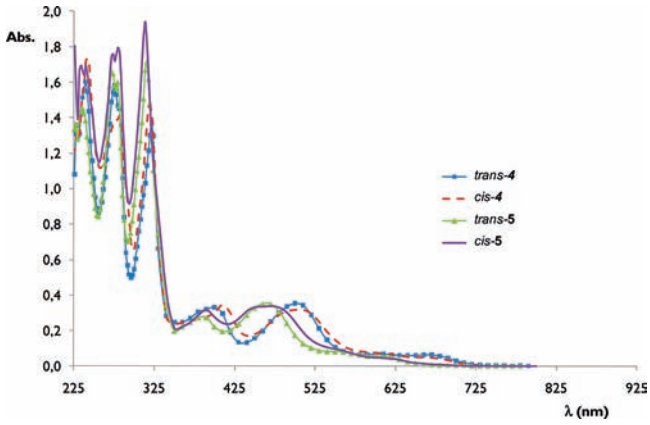

Figure 3. UV−vis spectra for complexes *trans*-**4**, *cis*-**4**, *trans*-**5**, and *cis*-**5**.

Redox Properties. The redox properties of the compounds have been determined by cyclic voltammetry (CV) and differential pulse voltammetry (DPV) experiments. Chlorocomplexes *trans*-**4** and *cis*-**4**, containing the neutral pypz-Me ligand, exhibit a reversible monoelectronic Ru(III/II) redox wave at around 0.8 V versus SSCE. On the other hand complex *trans*-**2**, with the anionic pyrrolate ligand, reaches the Ru(III) oxidation state at a much lower potential (0.21 V) as expected from the higher σ-donation arising from the negative charge of the pyrpy ligand. This sharp decrease of the $E_{1/2}$(III/II) value is similar to the one observed for analogous Ru complexes bearing neutral or anionic oxazoline ligands[15a] and, in the case of complex *trans*-**2**, this also allows the occurrence of the Ru(IV/III) redox couple within the CV range (at 0.79 V), which is a quite uncommon phenomenon for Ru(II) chlorocomplexes (see Supporting Information for additional electrochemical information).[16]

The redox properties of Ru-aqua complexes are pH dependent because of the capacity of the aqua ligand to lose protons upon oxidation of the complex, which also makes the upper oxidation states easily accessible:

$$[Ru^{II}(L)(trpy)(H_2O)]^{n+} \rightarrow [Ru^{III}(OH)(L)(trpy)]^{n+} + H^+ + e^- \quad (3)$$

$$[Ru^{III}(OH)(L)(trpy)]^{n+} \rightarrow [Ru^{IV}(O)(L)(trpy)]^{n+} + H^+ + e^- \quad (4)$$

The complete thermodynamic information regarding the Ru-aqua type of complex can be extracted from the Pourbaix diagrams, exhibited in Figure 4 for complex

(15) (a) Serrano, I.; Sala, X.; Plantalech, E.; Rodríguez, M.; Romero, I.; Jansat, S.; Gómez, M.; Parella, T.; Stoeckli-Evans, H.; Solans, X.; Font-Bardia, M.; Vidjayacoumar, B.; Llobet, A. *Inorg. Chem.* **2007**, *46*, 5381–5389. (b) Sala, X.; Santana, N.; Serrano, I.; Plantalech, E.; Romero, I.; Rodríguez, M.; Llobet, A.; Jansat, S.; Gómez, M.; Fontrodona, X.. *Eur. J. Inorg. Chem.* **2007**, 5207–5214. (c) Nishiyama, H.; Shimanda, T.; Itoh, H.; Sugiyama, H.; Motoyama, Y. *Chem. Commun.* **1997**, 1863–1864.

(16) Wasylenko, D. J.; Ganesamoorthy, C.; Koivisto, B. D.; Henderson, M. A.; Berlinguette, C. P. *Inorg. Chem.* **2010**, *49*, 2202–2209.

Table 2. pK_a and Electrochemical Data (pH = 7, $E_{1/2}$ in V vs SSCE) for the Aquocomplexes Described in This Work and Others for Purposes of Comparison

entry	complex[a] (trpy)(D)Ru-OH_2	$E_{1/2}$ (III/II)	$E_{1/2}$ (IV/III)	ΔE[b]	$E°$(IV/II)[c]	pK_a(II)	pK_a(III)	ref
1	(trpy)(bpy)Ru-OH_2	0.49	0.62	130	0.555	9.7	1.7	27a
2	*trans*-**3**	0.55[d]		<0	0.55	9.75	1.21	*e*
3	*trans*-**5**	0.39	0.57	180	0.48	10.1	0.95	*e*
4	*cis*-**5**	0.47	0.52	50	0.495	10.75	1.65	*e*
5	(trpy)(box-C)Ru-OH_2	0.48	0.60	120	0.54	>10	1.8	15a
6	(trpy)(box-O)Ru-OH_2	0.20				11.0	4.4	15a
7	*trans*-(trpy)(pic)Ru-OH_2	0.21	0.45	240	0.33	10.0	2	27b
8	*cis*-(trpy)(pic)Ru-OH_2	0.38	0.56	180	0.47	10.0	3.7	27b
9	(trpy)(acac)Ru-OH_2	0.19	0.56	370	0.375	11.2	5.2	18b

[a] D stands for didentate ligand, according to the following abbreviations: box-C = 4,4′-dibenzyl-4,4′,5,5′-tetrahydro-2,2′-bioxazole; box-O = 2-[((1′S)-1′-hydroxymethyl-2′-phenyl)ethylcarboxamide]-(4*S*)-4-benzyl-4,5-dihydrooxazole; pic = picolinate; acac = acetylacetonate. [b] $\Delta E = E_{1/2}$(IV/III) − $E_{1/2}$(III/II) in mV. [c] Average value calculated according to: $E°$(IV/II) = [$E_{1/2}$(IV/III) + $E_{1/2}$(III/II)]/2, in V. [d] $E_{1/2}$(IV/II) in V. [e] This work.

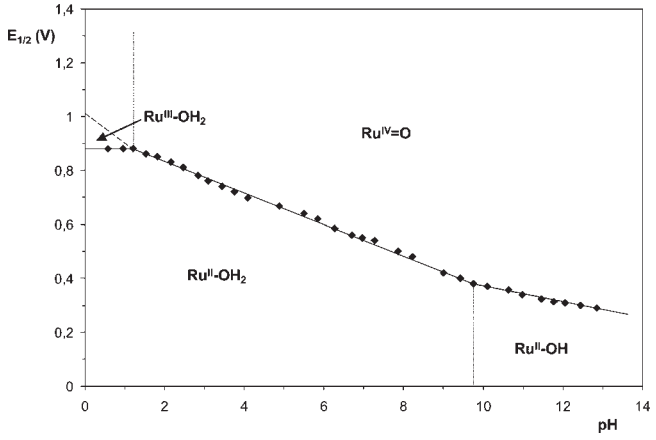

Figure 4. Pourbaix diagram of complex **3**. The pH-potential regions of stability for the various oxidation states and their dominant proton compositions are indicated.

trans-**3** and in Supporting Information, Figure S14 for complexes *trans*-**5** and *cis*-**5**.

Pourbaix diagram for complex *trans*-**3** shows a unique pH-dependent redox process throughout the whole pH range with a change in the slope value (from approximately 60 to 30 mV/pH unit) at pH around 9.7, a behavior that is generally indicative of the occurrence of a two-electron (IV/II) redox process. To confirm this point we have performed a redox spectrophotometric titration of the complex, both chemically (with Ce(IV) as oxidant) and electrochemically (through a controlled-potential electrolysis of a neutral aqueous solution of the complex at an applied potential of E = 0.57 V). In any case we obtained identical sets of spectra which are displayed in Supporting Information, Figure S12 for the electrochemical oxidation experiment. The presence of isosbestic points at 446, 362, and 337 nm indicates a net conversion from the initial to the final species that in both chemical and electrochemical experiments is obtained upon the transfer of 2 electrons. In contrast, pyrazole complexes *trans*-**5** and *cis*-**5** show two monoelectronic processes as indicated in eqs 2 and 3. For the *trans*-**5** isomer these two redox processes are clearly differentiated as displayed in the Pourbaix diagram (Supporting Information, Figure S14) whereas for complex *cis*-**5** an apparent single wave enclosing the two monoelectronic transfers is observed in CV experiments. Thus, we carried out a DPV experiment on *cis*-**5** and performed a mathematical deconvolution of the wave obtained, resulting in a 50 mV separation of the (IV/III) and (III/II) redox couples (see Supporting Information, Figure S15).

We also attempted to isolate the oxidized Ru^{IV}=O form of *trans*-**3** by adding 2 equiv of Ce^{IV} to an aqueous solution of the Ru(II) complex followed by addition of saturated aqueous NH_4PF_6. A yellow precipitate was initially obtained that nevertheless turned into a brown solid after a few minutes thus preventing its characterization. The extra stabilization of the Ru(IV) oxidation state gained thanks to the presence of the anionic pyrpy-O ligand is thus not sufficient to stabilize the oxo complex in the solid state, a fact that is in turn in agreement with the capability of the Ru^{IV}=O species to react in the presence of oxidizable substrates (see below the Catalytic Epoxidation section).

$E_{1/2}$ values at neutral pH for the three aquocomplexes described in this work are gathered in Table 2, together with additional electrochemical and pK_a data for other relevant Ru-trpy-aqua complexes previously reported in the literature for purposes of comparison. In all entries of Table 2, the notation *cis* or *trans* (to the aquo ligand) is referred to a ligand having higher σ-donor (or lower π-acceptor) capacity than a pyridyl ring.

A first look at Table 2 shows that complex *trans*-**3** is a particular case since it is the only one presenting a bielectronic wave. This characteristic seems to arise from a specific balance between σ-donor and π-acceptor properties of the ancillary ligands (as expressed by the Meyer−Lever plot[17]) and, in this case, the anionic pyrpy-O ligand looks appropriate to lead the Ru(III) state to disproportion. However, the ΔE value is not only governed by the ligands but also by the geometry of the complex. Thus, when comparing for instance entries 3 and 4, or 7 and 8 in Table 2 one can see that coordination of a relatively good σ-donor (or less π-acceptor) ligand in a *trans* fashion with respect to the aquo ligand lowers $E_{1/2}$(III/II) with respect to the analogous *cis* isomer hence stabilizing the Ru(III) species.[18] The Ru(IV/III) redox potential is also affected when comparing isomeric picolinate complexes but to a much lesser extent in the case of *trans*-**5** and *cis*-**5**. This could be a consequence of the steric encumbrance of the methyl group of the pypz-Me ligand. These data illustrate how the electron density is more effectively transmitted to the metal center in a *trans*

(17) Lever, A. B. P. *Inorg. Chem.* **1990**, *29*, 1271.
(18) (a) Leising, R. A.; Takeuchi, K. J. *Inorg. Chem.* **1987**, *26*, 4391–4393. (b) Bessel, C. A.; Leising, R. A.; Takeuchi, K. J. *J. Chem. Soc; Chem. Commun.* **1991**, 883–835.

Table 3. Catalytic Epoxidation Performance of *trans*-**3**, *trans*-**5**, and *cis*-**5** for the Epoxidation of a Variety of Alkenes Using $PhI(OAc)_2$ as Oxidant[a]

		complex								
		trans-**3**			*trans*-**5**			*cis*-**5**		
entry	alkene	conversion (%)	selectivity (%)[b]	ν_i[c]	conversion (%)	selectivity (%)	ν_i	conversion (%)	selectivity (%)	ν_i
1	styrene	80	62	6.3	43	96.5	3.4	72	84	5.3
2	*trans*-stilbene	>99[e]	86	10.8	96	84	6.0	47	79	2.9
3	*cis*-β-methylstyrene[d]	55	69	3.7	90	99	7.9	>99	86	7.9
4	cyclooctene	>99	>99		>99	>99		>99	>99	
5	1-octene	30	>99	1.6	53	97	2.7	10	90	
6	4-vinylcyclohexene[f]	55	87	4.2	84	74	7.6	85	96	8.3

[a] Conditions: alkene (50 mM), complex (0.5 mM), oxidant $PhI(OAc)_2$ (100 mM), CH_2Cl_2 (2.5 mL), 25 °C, 24 h, biphenyl (15 mM) as internal standard. [b] Selectivity for epoxide, (Yield/Conversion) × 100. [c] ν_i is defined as initial rate for substrate consumption (expressed in 10^{-6} mol·h^{-1}). [d] % of *cis*-epoxide: complex **3,** 100%; complex *trans*-**5,** 98%; complex *cis*-**5,** 97%. [e] Analysis performed after 15 h. [f] Epoxidation on the cyclohexene ring.

fashion with regard to the aqua group than in *cis*, and it is also interesting to note that this is a particular feature of aquocomplexes since the corresponding *trans*-**4** and *cis*-**4** chlorocomplexes display almost identical $E_{1/2}$(III/II) values.

Also, for a given *trans* or *cis* geometry, anionic ligands (i.e., entries 6, 7, and 9) in general decrease the redox potentials with regard to neutral ligands (entries 1, 3, and 5). Complex **3** appears as an exception to this trend but this might be due to the oxidation of the initial pyrpy ligand which would make it a worse σ-donor as the corresponding chlorocomplex **2** displays clearly lower $E_{1/2}$(III/II) redox potential than both isomer complexes **4**.

Catalytic Epoxidations. The catalytic activity of the ruthenium aquocomplexes *trans*-**3**, *trans*-**5**, and *cis*-**5** was investigated in the epoxidation of a diversity of alkenes using different oxidants, given the interest of the epoxidation reaction in both bulk and fine chemicals, that use them as starting materials for a variety of reactions.[19]

Initial essays were performed with styrene and *trans*-stilbene as test substrates using complex *trans*-**3** as catalyst and varying solvents and oxidants and the results are reported in the Supporting Information. Optimal reactivity was achieved with the following conditions: CH_2Cl_2 as solvent; $PhI(OAc)_2$ as oxidant; catalyst/substrate/oxidant molar ratio of 1:100:200. These conditions were then used to test all substrates with the three aquocomplexes, *trans*-**3**, *trans*-**5**, and *cis*-**5**, and their performance is gathered in Table 3. No epoxidation occurred in the absence of catalyst in any case.

Complexes *trans*-**3**, *trans*-**5**, and *cis*-**5** constitute an excellent ground to study the influence of electronic and steric effects on the Ru(IV)═O group with regard to the epoxidation of olefins. It is interesting to realize here that complex *trans*-**3** containing the anionic pyrpy ligand has the highest $E°$(IV/II) redox potential 0.55 V, compared to 0.48 and 0.495 V for the complexes containing the neutral pypz-Me ligand *trans*-**5** and *cis*-**5**, respectively (see Table 3). On the other hand it is also interesting to bear in mind the spatial arrangement of the ligands close to the Ru═O active group where the olefin will approach. The

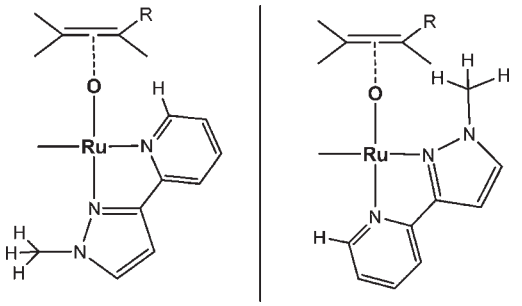

Figure 5. Drawing showing the steric interactions for the *cis*/*trans* **5** scenarios with the approaching substrate (trpy ligand is situated perpendicular to the pypz-Me ligand and has been omitted for clarity purposes).

trans-**3** and *trans*-**5** complexes contain a pyridine C−H bond nearly parallel to the Ru−O bond whereas in sharp contrast for *cis*-**5** this position is occupied by a C-Me group and thus will exert a much stronger steric effect (see Figure 5).

For the case of styrene (entry 1, Table 3), where in our particular set of complexes steric effects will not play major role, electronic effects are expected to strongly dominate the reactivity. Indeed we observe a strong correlation with redox potentials; thus the higher the $E°$(IV/II) the higher the efficiencies obtained (*trans*-**3** > *cis*-**5** > *trans*-**5**). Steric effects are expected to play an important role for the case of *trans*-stilbene, and this is exactly what we observed as reflected in the entry 2 of Table 3. Complexes *trans*-**3** and *trans*-**5** are very active toward the epoxidation of *trans*-stilbene with high initial consumption rates ν_i, and practically complete conversion whereas the ν_i and conversion for the sterically hindered *cis*-**5** drops substantially manifesting the combination of electronic and steric effects. The activity of catalysts *trans*-**3**, *trans*-**5**, and *cis*-**5** was also tested with regard to their capacity to epoxidize *cis*-β-methyl-styrene (entry 3, Table 3). Complexes containing the pypz-Me ligand perform much better than the one containing the pyrpy ligand, and it is striking to see that in all cases the isomerization to the *trans*-epoxide is practically nonexistent. This is in agreement with a potential O-atom transfer concerted mechanism, which is in turn consistent with the low stability of Ru(III) that favors 2e- versus

(19) (a) Smith, J. G. *Synthesis* **1984**, 629–656. (b) Schneider, C. *Synthesis-Stuttgart* **2006**, 3919–3944. (c) Weissermel, K. *Industrial Organic Chemistry*, 3rd ed.; VCH: Weinheim, 1997. (d) Xia, Q.-H.; Ge, H.-Q.; Ye, C.-P.; Liu, Z.-M.; Su, K.-X. *Chem. Rev.* **2005**, *105*, 1603. (e) Che, C.-M.; Huang, J.-S. *Chem. Commun.* **2009**, 3996–4015. (f) Chatterjee, D. *Coord. Chem. Rev.* **2008**, *252*, 176–198. (g) Gupta, K. C.; Sutar, A. K.; Linb, C.-C. *Coord. Chem. Rev.* **2009**, *253*, 1926–1946.

(20) (a) Masllorens, E.; Rodríguez, M.; Romero, I.; Roglans, A.; Parella, T.; Benet-Buchholz, J.; Poyatos, M.; Llobet, A. *J. Am. Chem. Soc.* **2006**, *128*, 5306–5307. (b) Yu, X.-Q.; Huang, J.-S.; Che, C.-M. *J. Am. Chem. Soc.* **2000**, *122*, 5337–5342.

1e- transfer process (see ΔE values in Table 2).[20] This is an interesting and relevant phenomenon to be controlled since Mn-salen complexes generally yield a mixture of *cis*/*trans* isomerization epoxides.[21] It is also very interesting to compare the activity of our catalysts with regard to styrene (entry 1, Table 3) and cis-β-methylstyrene (entry 3, Table 3). For complexes *cis*-**5** and *trans*-**5** the ν_i significantly increases when comparing the oxidation of styrene versus *cis*-β-methylstyrene whereas the opposite effect takes place in the case of *trans*-**3**. This clearly suggests that for *cis*-**5** and *trans*-**5** the Ru=O has strong electrophilic character whereas for *trans*-**3** the Ru=O group displays the opposite effect. This result is in agreement with the relative value of the Ru(IV)/Ru(II) redox potentials obtained for these complexes and puts forward the strong ligand influence into the nature and reactivity of the Ru=O active group. It is pertinent to mention here that in general related Mn complexes such as $Mn(phen)_x$ (x = 1 or 2; phen is phenathroline)[22] present mainly an electrophilic character. It is also interesting to see here that catalysts *cis*- and *trans*-**5** containing the more σ-donating pyrazole ligand display much better performances than their homologues containing pyridylic or imidazole type of ligands only.[23]

The ability of the catalysts was also tested with aliphatic substrates. With cyclooctene we obtain complete conversion with our catalysts (entry 4, Table 3) and with 1-octene we have modest to low performances with all three catalysts in agreement with their lower reactivity toward unactivated monosubstituted alkenes. Finally the catalysts show activity toward the ring epoxidation of 4-vinylciclohexene with again better performances for the *trans*-**5** and *cis*-**5** that have lower redox potentials than *trans*-**3** which again is in agreement with the electrophilic character of the former.

In conclusion, we have synthesized and characterized a new family of Ru-OH_2 complexes where the ligand design strongly influences sterics and electronics as evidenced by their spectroscopic and redox properties. This is in turn manifested by the reactivity of these complexes toward the epoxidation of a series of aromatic and aliphatic alkenes.

Experimental Section

Materials. All reagents used in the present work were obtained from Aldrich Chemical Co and were used without further purification. Reagent grade organic solvents were obtained from SDS and high purity deionized water was obtained by passing distilled water through a nanopure Mili-Q water purification system. $RuCl_3 \cdot 2H_2O$, was supplied by Johnson and Matthey Ltd. and was used as received.

Preparations. Ligands pyrpy (3,5-dimethyl-2-(2-pyridyl)pyrrole)[24] and pypz-Me (2-(1-Methyl-3-pyrazolyl)pyridine)[25] (Scheme 1) and the complexes $[Ru^{III}Cl_3(trpy)]$, **1**[26] (trpy is 2,2′:6′,2″-terpyridine), were prepared as described in the literature. All synthetic manipulations were routinely performed under nitrogen atmosphere using Schlenk tubes and vacuum line techniques. Electrochemical experiments were performed under either N_2 or Ar atmosphere with degassed solvents.

***trans*-[Ru^{II}Cl(pyrpy)(trpy)]·0.3$CHCl_3$, *trans*-2·0.3$CHCl_3$.** A sample of **1** (0.2 g, 0.45 mmol) was added to a 250 mL round bottomed flask containing a solution of LiCl (0.057 g, 1.36 mmol) dissolved in 85 mL of EtOH (96%), under magnetic stirring. Then NEt_3 (0.25 mL, 1.73 mmol) was added, and the reaction mixture was stirred at room temperature for 30 min. Next pyrpy (0.077 g, 0.45 mmol) together with NEt_3 (0.1 mL, 0.7 mmol) dissolved in EtOH was added, and the mixture was heated at reflux for 3 h. The solution was then cooled and filtered off in a frit. A dark solid was obtained that was recrystallized from $CHCl_3$/diethyl ether obtaining the violet chlorocomplex **2**. Yield: 0.1 g (41.1%). Anal. found (calcd) for $C_{26}H_{22}N_5ClRu \cdot 0.3CHCl_3$: C, 54.74 (54.76); N, 11.73 (12.14); H, 4.34 (3.90). ^{1}H NMR (600 MHz, acetone-d_6) δ (ppm): 9.91 (d, H16), 8.52 (d, H7, H9), 8.44(d, H1, H15), 7.90 (d, H4, H12), 7.82 (m, H8), 7.81(m, H2, H14), 7.77 (t, H18), 7.66 (d, H19), 7.34 (t, H3, H13), 7.06 (t, H17), 5.11 (s, H23), 2.3(s, H25, Me), 0.96 (s, H26, Me). For the NMR assignment we have used the same numbering scheme as for the X-ray displayed in Figure 1. IR (ν_{max}, cm^{-1}): 1594 (m), 1481 (m),1355 (m), 1276 (m), 971 (s), 632 (m). $E_{1/2}$(III/II) = 0.21 V, $E_{1/2}$(IV/III) = 0.79 V versus SSCE. UV−vis (CH_2Cl_2):- λ_{max}, nm (ε, M^{-1} cm^{-1}) 240 (13670), 278 (11490), 320 (19390), 540(3050).ESI-MS (m/z): 541.1 [M + H^+].

***trans*-[Ru^{II}(pyrpy-O)(trpy)]OH_2](PF_6), *trans*-3.** A sample of $AgNO_3$ (0.031 g, 0.184 mmol) was added to a solution of acetone/H_2O (1:2) (30 mL) containing **2** (0.050 g, 0.092 mmol) and heated at reflux for 2 h. After cooling the precipitated AgCl was filtered off through a frit containing Celite. Afterward NH_4PF_6 (1 mL) was added to the filtrate, and the volume reduced in a rotary evaporator. A precipitate appeared that was washed with cold water (3 × 5 mL). Yield: 0.045 g (71%). ^{1}H NMR (600 MHz, D_2O) δ (ppm): 9.49 (d, H16), 8.56 (d, H19), 8.41(d, H7), 8.36 (d, H9), 8.32 (d, H12), 8.24 (d, H4), 8.19 (t, H18), 8.05 (t, H8), 7.95 (t, H17), 7.93 (t, H13), 7.87 (t, H3), 7.51 (d, H15), 7.38 (d, H1) 7.29 (t, H14), 7.22 (t, H2), 1.89 (s, H25), 0.23 (s, H26). IR (ν_{max}, cm^{-1}): 3654 (m), 1606 (m), 1450 (m), 1288 (w), 836 (s), 554 (m). $E_{1/2}$ (IV/II), phosphate buffer pH = 7: 0.55 V versus SSCE. UV−vis (phosphate buffer pH = 7): λ_{max}, nm (ε, M^{-1} cm^{-1}) 271 (11960), 311 (11580), 511 (4000). ESI-MS (m/z): 540.1 [M − PF_6^-].

***trans* and *cis*-[Ru^{II}Cl(pypz-Me)(trpy)](PF_6), *trans*-4 and *cis*-4·0.8CH_2Cl_2.** A sample of **1** (0.150 g, 0.22 mmol) was added to a 100 mL round bottomed flask containing a solution of LiCl (0.018 g, 0.44 mmol) dissolved in 40 mL of EtOH/H_2O (3:1), under magnetic stirring. Then, NEt_3 (0.06 mL, 0.42 mmol) was added, and the reaction mixture was stirred at room temperature for 30 min. Afterward pypz-Me (0.052 g, 0.218 mmol) was added and heated at reflux for 3 h. The hot solution was then filtered off in a frit, and a saturated aqueous solution of NH_4PF_6 (1.5 mL) was added. After reduction of the volume in a rotary evaporator a precipitate formed that was filtered off and washed several times with water. The solid obtained in this manner was a mixture of complexes *trans*-**4** and *cis*-**4** that can be separated by column chromatography (silica; CH_2Cl_2/acetone 90:10). Both chlorocomplexes were recrystallized from CH_2Cl_2/ether, and the resulting precipitates were filtered on a frit, washed with a small amount of ether and pentane, and dried under vacuum. For *trans*-**4:** yield, 0.042 g (28.5%). Anal. Found (Calcd) for $C_{24}H_{20}N_6ClRuPF_6$: C, 42.62 (42.77); N, 12.15 (12.47); H, 2.85 (2.99). ^{1}H NMR (600 MHz, acetone-d_6) δ (ppm): 10.20 (dt, H16), 8.73 (d, H7, H9), 8.61 (dt, H4, H12), 8.50 (dt, H19), 8.32

(21) (a) Jacobsen, E. N.; Zhang, W.; Güler, M. L. *J. Am. Chem. Soc.* **1991**, *113*, 6703–6704. (b) Cavallo, L.; Jacobsen, H. *J. Org. Chem.* **2003**, *68*, 6202–6207.
(22) Terry, T. J.; Stack, T. D. *J. Am. Chem. Soc.* **2008**, *130*, 4945–4953.
(23) (a) Hamelin, O.; Menage, S.; Charnay, F.; Chavarot, M.; Pierre, J. L.; Pécaut, J.; Fontecave, F. *Inorg. Chem.* **2008**, *47*, 6413–6420. (b) Murali, M.; Mayilmurugan, R.; Palaniandavar, M. *Eur. J. Inorg. Chem.* **2009**, 3238–3249.
(24) Bolm, C.; Weickhardt, K.; Zehnder, M.; Glasmacher, D. *Chem. Ber.* **1991**, *124*, 1173–1180.
(25) Huckel, W.; Bretschneider, H. *Chem. Ber.* **1937**, *9*, 2024.
(26) Sullivan, B. P.; Calvert, J. M.; Meyer, T. J. *Inorg. Chem.* **1980**, *19*, 1404–1407.
(27) (a) Binstead, R. A.; Meyer, T. J. *J. Am. Chem. Soc.* **1987**, *109*, 3287–3297. (b) Llobet, A.; Doppelt, P.; Meyer, T. J. *Inorg. Chem.* **1988**, *27*, 514–520.

(td, H18), 8.17 (t, H8), 8.00 (td, H3, H13), 7.88 (td, H17), 7.84 (ddd, H1, H15), 7.59 (d, H22), 7.45 (td, H2, H14), 7.21 (d, H23), 3.05 (s, H24). IR (ν_{max}, cm^{-1}): 1619 (w), 1450 (m), 1251 (w), 833 (s), 761 (m), 555 (m). $E_{1/2}(CH_2Cl_2) = 0.79$ V versus SSCE. UV−vis (CH_2Cl_2): λ_{max}, nm (ε, M^{-1} cm^{-1}) 239 (15960), 274 (15650), 321 (13660), 400(3300), 501 (3550).

For *cis*-**4**, yield: 0.038 g (26%). Anal. Found (Calcd) for $C_{24}H_{20}N_6ClRuPF_6 \cdot 0.8CH_2Cl_2$: C, 40.10 (40.15); N, 11.56 (11.32); H, 3.03 (2.93). ^{1}H NMR (600 MHz, acetone-d_6) δ (ppm): 8.69 (d, H7,H9), 8.59 (dt, H4, H12), 8.43 (d, H22), 8.18 (ddd, H19), 8.17 (t, H8), 8.09 (ddd, H1, H15), 8.00 (td, H3, H13), 7.72 (td, H18), 7.59 (d, H23), 7.47 (td, H2,H14), 7.37(ddd, H16), 6.96 (td, H17), 4.76 (s, H24). IR (ν_{max}, cm^{-1}): 1627 (w), 1448 (m), 1253 (w), 833 (s), 763 (m), 555 (w). $E_{1/2}(CH_2Cl_2) = 0.80$ V versus SSCE. UV−vis (CH_2Cl_2): λ_{max}, nm (ε, M^{-1} cm^{-1}) 241 (17260), 280 (14130), 318 (14640), 409 (3440), 499 (3180). For the NMR assignment we have used the same numbering scheme as for the X-ray displayed in Figure 1.

***trans*-[Ru^{II}(pypz-Me)(trpy)OH_2]$(PF_6)_2 \cdot H_2O$, *trans*-5$\cdot H_2O$.** A sample of $AgNO_3$ (0.017 g, 0.102 mmol) was added to a solution of H_2O (15 mL) containing *trans*-**4** (0.035 g, 0.051 mmol) and heated at reflux for 3 h in absence of light. AgCl was filtered off through a frit containing Celite. Afterward NH_4PF_6 saturated aqueous soluton (1 mL) was added, and the product was precipitated upon reduction of volume in a rotary evaporator. The green solid obtained was then filtered and washed with ether and pentane and dried under vacuum. Yield: 0.030 mg (73.4%). Anal. Found (Calcd) for $C_{24}H_{22}N_6ORuP_2F_{12} \cdot H_2O$: C, 34.82 (35.10); N, 10.05 (10.23); H, 2.62 (2.97). ^{1}H NMR (600 MHz, acetone-d_6/10% D_2O) δ (ppm): 9.58 (d, H16), 8.84 (d, H7, H9), 8.68 (d, H4, H12), 8.54 (d, H19), 8.37 (t, H18), 8.33 (t, H8), 8.10 (t, H3, H13), 7.97 (t, H17), 7.92 (d, H1, H15), 7.58 (d, H22), 7.52 (t, H2, H14), 7.22 (d, H23), 3.05 (s, H24). $E_{1/2}$ (III/II), phosphate buffer pH = 7: 0.39 V; IR (ν_{max}, cm^{-1}): 3478 (w), 3342 (m), 1623 (m), 1448 (m), 1251 (w), 827 (s), 763 (s), 555 (s). $E_{1/2}$ (IV/III): 0.57 V versus SSCE. UV−vis (phosphate buffer pH = 7): λ_{max}, nm (ε, M^{-1} cm^{-1}) 229 (16460), 271 (17620), 313 (18520), 381 (3100), 459 (3810).

***cis*-[Ru^{II}(pypz-Me)(trpy)OH_2]$(PF_6)_2 \cdot H_2O$, *cis*-5$\cdot H_2O$.** A sample of $AgNO_3$ (0.021 g, 0.12 mmol) was added to a solution of H_2O (15 mL) containing *cis*-**4** (0.040 mg, 0.06 mmol) and heated at reflux for 3 h in absence of light. AgCl was filtered off through a frit containing Celite. Afterward NH_4PF_6 saturated aqueous solution (1 mL) was added, and the product was precipitated from the resulting solution after reduction of volume in a rotary evaporator. The brown solid obtained was then filtered and washed with ether and pentane and dried under vacuum. Yield: 0.025 mg (52%). Anal. Found (Calcd) for $C_{24}H_{22}N_6ORuP_2F_{12} \cdot 1.3CH_2Cl_2$: C, 34.94 (33.32); N, 9.62 (9.21); H, 2.67 (2.71). ^{1}H NMR (600 MHz, acetone-d_6/10% OD_2) δ (ppm): 8.78 (d, H7, H9), 8.65 (d, H4, H12), 8.46 (d, H23), 8.31 (t, H8), 8.16 (d, H1, H15), 8.14 (d, H19), 8.09 (td, H3, H13), 7.71 (td, H17), 7.58 (d, H23), 7.53 (td, H2,H14), 7.32(d, H16), 6.94 (td, H17), 4.56 (s, H24). IR (ν_{max}, cm^{-1}): 3494 (m), 1630 (w), 1450 (m), 1247 (w), 831 (s), 765 (s), 555 (s). $E_{1/2}$ (III/II), phosphate buffer pH = 7: 0.47 V; $E_{1/2}$ (IV/III): 0.52 V versus SSCE. UV−vis (phosphate buffer pH = 7): λ_{max}, nm (ε, M^{-1} cm^{-1}) 231 (24380), 269 (23330), 311 (28520), 387 (4390), 455 (4940).

Instrumentation and Measurements. UV/vis spectroscopy was performed on a Cary 50 Scan (Varian) UV/vis spectrophotometer with 1 cm quartz cells. CV and DPV experiments were performed in a IJ-Cambria IH-660 potentiostat using a three electrode cell. Glassy carbon electrodes (3 mm diameter) from BAS were used as working electrode, platinum wire as auxiliary, and SSCE as the reference electrode. All cyclic voltammograms presented in this work were recorded under nitrogen atmosphere. All $E_{1/2}$ values estimated from CV were calculated as the average of the oxidative and reductive peak potentials $(E_{pa} + E_{pc})/2$ at a scan rate of 100 mV/s whereas they were directly taken from the maximum of the peak in DPV experiments. Unless explicitly mentioned the concentration of the complexes were approximately 1 mM. In aqueous solutions the pH was adjusted from 0 to 2 with 5 M HCl. Potassium chloride was added to keep a minimum ionic strength of 0.1 M. From pH 2−10, 0.1 M phosphate buffers were used, and from pH 10−12 diluted, CO_2 free, NaOH. Bulk electrolyses were carried out in a three-compartment cell using carbon felt from SOFACEL as the working electrode.

The ^{1}H NMR spectroscopy was carried out on a a Bruker DPX 200 MHz or a Bruker 600 MHz. Samples were run in acetone-d_6 or $CDCl_3$, with internal references (residual protons and/or tetramethylsilane). Elemental analyses were performed using a CHNS-O Elemental Analyzer EA-1108 from Fisons. ESI-MS experiments were performed on a Navigator LC/MS chromatograph from Thermo Quest Finnigan, using acetonitrile as a mobile phase.

For acid−base spectrophotometric titration, $3-4 \times 10^{-5}$ M buffered aqueous solutions of the complexes were used. The pH of the different solutions was adjusted by adding small volumes (approximately 5 μL) of 7 M NaOH to produce a negligible overall volume change. Redox spectrophotometric titrations were performed by sequential addition of a $(NH_4)_2[Ce^{IV}(NO_3)_6]$ 0.1 M solution in HCl to the complex.

X-ray Structure Determination. Measurement of the crystals were performed on a Bruker Smart Apex CCD diffractometer using graphite-monochromated Mo Kα radiation ($\lambda = 0.71073$ Å) from an X-ray tube. Data collection, Smart V. 5.631 (BrukerAXS 1997−02); data reduction, Saint+ Version 6.36A (Bruker AXS 2001); absorption correction, SADABS version 2.10 (Bruker AXS 2001) and structure solution and refinement, SHELXTL Version 6.14 (Bruker AXS 2000−2003). The crystallographic data as well as details of the structure solution and refinement procedures are reported in Table 1 and Supporting Information, Table S1. CCDC 781563 (*trans*-**2**), 781564 (*trans*-**4**), and 781565 (*cis*-**4**) contain the supplementary crystallographic data for this paper. These data can be obtained free of charge from The Cambridge Crystallographic Data Centre via www.ccdc.cam.uk/data_request/cif.

Catalytic Studies. Experiments have been performed in anhydrous dichloromethane at room temperature. In a typical run, Ru catalyst (0.5 mM), alkene (50 mM), and $PhI(OAc)_2$ (100 mM) were stirred at room temperature in dichloromethane (2.5 mL) for 24 h. The end of the reaction was indicated by the disappearance of solid co-oxidant. After the addition of an internal standard, an aliquot was taken for gas chromatographic (GC) analysis. The oxidized products were analyzed in a Shimadzu GC-17A gas chromatography apparatus with a TRA-5 column (30 m × 0.25 mm diameter) incorporating a flame ionization detector. GC conditions: initial temperature, 80 °C for 10 min; ramp rate, 10 °C min^{-1}; final temperature, 220 °C; injection temperature, 220 °C; detector temperature, 250 °C; carrier gas, He at 25 mL min^{-1}. All catalytic oxidations were carried out under a N_2 atmosphere.

Acknowledgment. This research has been financed by MICINN of Spain (CTQ2007-60476/PPQ, CTQ2007-67918) and Consolider Ingenio 2010 (CSD2006-0003)). Johnson & Matthey LTD are acknowledged for a $RuCl_3 \cdot nH_2O$ loan. M.D. thanks AECID (MAEC) of Spain for the allocation of a MAEC-AECID grant.

Supporting Information Available: Additional information in the form of Tables S1−S5 and Figures S1−S16 and crystallographic data in CIF format. This material is available free of charge via the Internet at http://pubs.acs.org.